

# In-situ energy calibration of SSRF macromolecular crystallography beamline using powder diffraction

TAO Shixing<sup>1,2</sup> ZHU Jing<sup>1</sup> NIU Jing<sup>1</sup> CHEN Mingzhi<sup>1</sup> LIU Ke<sup>1</sup> WANG Yu<sup>1</sup>  
WANG Qisheng<sup>1</sup> SUN Bo<sup>1</sup> HUANG Sheng<sup>1</sup> TANG Lin<sup>1</sup> HE Jianhua<sup>1,\*</sup>

<sup>1</sup>Shanghai Institute of Applied Physics, Chinese Academy of Sciences, Shanghai 201800, China

<sup>2</sup>Graduate University of Chinese Academy of Sciences, Beijing 100049, China

**Abstract** For X-ray powder diffraction spectra collected by an area detector of MarCCD on macromolecular crystallography beamline of SSRF, an energy calibration method was developed using LaB<sub>6</sub>(660a) powder diffraction for *in-situ* rapid energy calibration of the X-rays without changing the experimental conditions. The intensity of each diffraction ring was integrated, and the accurate peak positions were fitted by Pseudo-Voigt function model. The sample's interplanar spacing for XRD analysis and the calibrated energy were obtained by the PCPDFWIN code and by fitting all the energies with the least-square method. The exposure time and the sample-to-detector distance were found no effect on accuracy of the energy calibration, and the *in-situ* energy calibration could be done with an accuracy of better than 0.4‰ in 7–18 keV. This method is applicable to other X-ray beamlines.

**Key words** X-ray, Energy calibration, Powder diffraction, Beamline.

## 1 Introduction

Based on an undulator inserted on a straight section of the SSRF storage ring, the macromolecular crystallography beamline provides high-brightness monochromatic X-ray beams. The experiments on the beamline, including multiple-wavelength anomalous diffraction (MAD) and single-wavelength anomalous diffraction (SAD), request precise energy calibration of the incident X-rays. Usually, by setting the Bragg angle of the silicon crystal of the monochromator, an X-ray energy can be calculated by the Bragg equation. However, the calculation result may deviate from its actual value due to thermal deformation of the crystal and errors in calibrating the reference position. In addition, many experiments need to a quick energy calibration.

The X-ray energy calibration can be done by measuring of the extended X-ray absorption fine structure spectroscopy (EXAFS) with a standard sample<sup>[1]</sup>, the Bragg angle of the analyzer crystal<sup>[2]</sup>, or

the X-ray flux at different azimuthal angles of the crystal<sup>[3]</sup>. The standard powder of Si640b<sup>[4]</sup> and the FIT2D code<sup>[5]</sup> are often used in powder diffraction experiments, and energy calibration at particular energies is performed with the absorption edge of metal elements. Nevertheless, the macromolecular crystallography experimental station has little room to allow installation of a diffractometer. Using multiple X-ray diffraction, a complicated practice though, one can calibrate a few energy points, but the Si640b standard powder has a precision of only several eVs. In view of all these, We used the powder of LaB<sub>6</sub>(660a) for *in-situ* energy calibration of the beamline, because the diffraction spectra are suitable for the fast and convenient energy calibration without changing any component of the beamline, and the LaB<sub>6</sub> powder is of high hardness, strength, and chemical stability<sup>[6–8]</sup>.

## 2 Theory

Fig.1 is a scheme of the energy calibration. The diffraction patterns are collected by a MarCCD of

Supported by Shanghai Natural Science Foundation (No.08JC1422500); National Natural Science Foundation of China (No.10774155)

\* Corresponding author. E-mail address: hejianhua@sinap.ac.cn

Received date: 2010-05-17

73- $\mu\text{m}$  pixel size. The angular step ( $\Delta 2\theta$ ) of each pixel is given by Eq. (1),

$$\Delta 2\theta = (180/\pi)[0.073 \cos^2(2\theta)]/l \quad (1)$$

where,  $2\theta$  is the diffraction angle, and  $l$  is sample-to-MarCCD distance at  $2\theta$ .

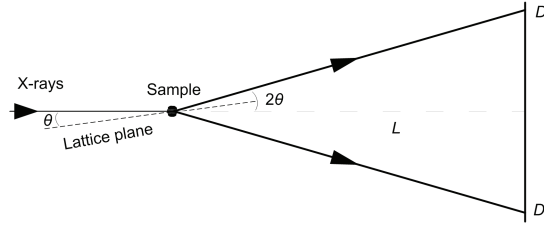


**Fig.1** Geometry of the energy calibration.

In Fig.2, the angular resolution ( $1/\Delta 2\theta$ ) increases with  $l$  and  $2\theta$ , with higher  $1/\Delta 2\theta$  at larger  $l$ . In the high energy region, 13 circular diffraction patterns are taken and fitted due to the weak diffraction intensity of  $\text{LaB}_6$  in the high-index crystal plane, while in the low-energy region, of short distance, less than 13 diffraction circles can be collected, with the  $1/\Delta 2\theta$  being good enough for energy calibration, because the wide Darwin width of the monochromator crystal has a linear relation with the angular intensity distribution of an incident X-ray.

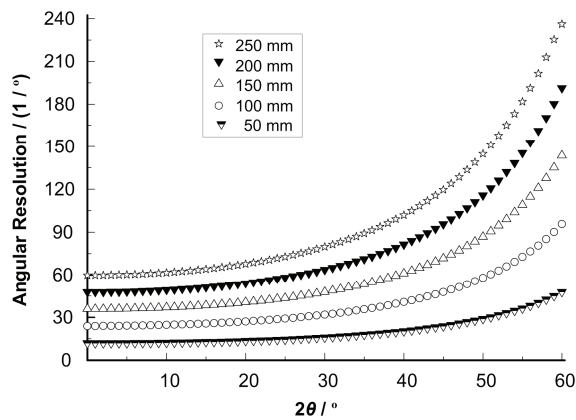


**Fig.2** Angular resolution as a function of diffraction angle at different sample-to-detector distances.

## 2.1 Diffraction peak fitting and its FWHM

The Pseudo-Voigt function model<sup>[7]</sup>, which describes the peak profile as a combination of a Lorentz ( $L$ ) with a Gaussian ( $G$ ) peak shape function, is used to fit the diffraction peak by,

$$PV = \eta L + (1-\eta)G \quad (2)$$

where,  $\eta$  describes ratio of the Lorentz part, which increases with  $2\theta$ <sup>[7]</sup>. The peak profiles are almost pure Gaussian at low angles. FWHM of the X-ray energy depends on the divergence angle of incident X-ray ( $\alpha$ ), Darwin width of monochromator crystal ( $\omega$ ), sample diameter ( $p$ ), and sample-to-MarCCD distance ( $l$ ), as given in Eq.(3). Fig.3 shows that the Darwin width decreases rapidly with increasing energies of the incident X-rays.

$$\begin{aligned} \text{FWHM}(2\theta) &\approx (180/\pi)[1/\cos(2\theta+0.5\alpha)-1/\cos(2\theta \\ &-0.5\alpha)+p/l]\omega\cos^2(2\theta) \end{aligned} \quad (3)$$

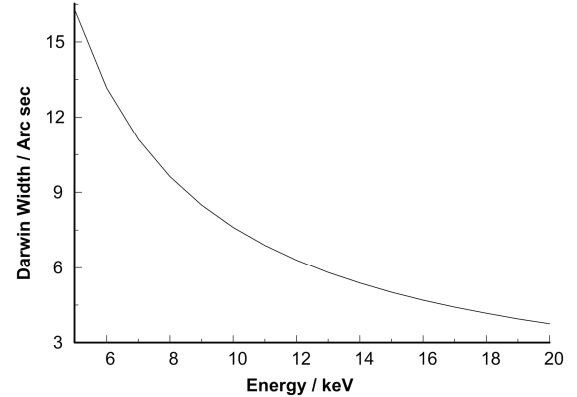


**Fig.3** Darwin width of monochromatic X-ray as a function of X-ray energy.

The diffraction intensity of each crystal plane is obtained by its ring integration. The exposure time is as long as possible, without saturating the MarCCD pixels, to achieve larger peak areas, without disturbing the peak position and the calibration result, as shown in Fig.4.

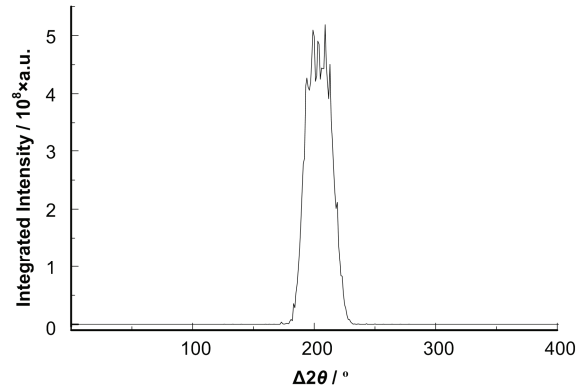


**Fig.4** No obvious diffraction peaks for 20-s exposure time.

## 2.2 The center of diffraction circle and its radius

The wavelength ( $\lambda$ ) is given by the Bragg equation,

$$2d_i \sin(\theta_i) = \lambda \quad (4)$$

$$\tan(2\theta_i) = r_i/l \quad (5)$$

where,  $d_i$  is the interplanar spacing and  $r_i$  is radius of the  $i^{\text{th}}$  diffraction circle. Eqs.(6) and (7) are applicable to two rings ( $i, j$ ).

$$\sin[0.5 \arctan(r_i/l)]/\sin[0.5 \arctan(r_j/l)] = d_j/d_i \quad (6)$$

$$2d_j \sin[0.5 \arctan(r_i/l)] = \lambda_{ij} \quad (7)$$

where, the actual  $\lambda$ , which is only related to  $r$ , is generally got from a series of  $\lambda_{ij}$  using the least square method.

### 2.2.1 Remove the background noise

The gray scale of diffraction spectra ranges from zero to tens of thousands. By displaying all the points of the same brightness, the diffraction circles are shown in Fig.5(a), but there are a number of background points, which would affect the fitting accuracy. Given a maximal gray value of  $I$ , and the background points can be removed to 0.0005 $I$  gray value, Fig.5(b) shows the modified diffraction spectra.

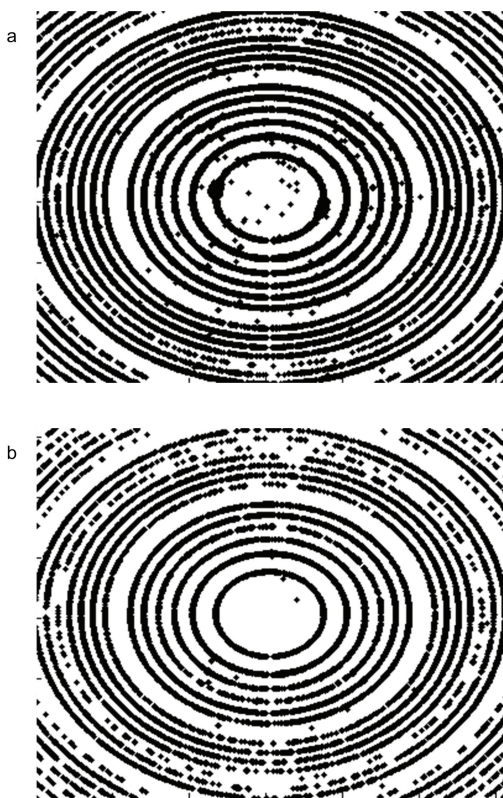


**Fig.5** Diffraction pattern for points of the same brightness (a) and the background points-removed pattern (b).

### 2.2.2 Refine the radius of the diffraction circle

The center ( $c$ ) and the radius ( $r$ ) of each diffraction circle are extracted approximately with the coordinate of all points and solved by the linear equations. Without considering the gray value of the points, the diffraction peaks and positions are obtained by integrating their intensity, and the peak profile is fitted by the Pseudo-Voigt function model to amend the  $r$ .

## 3 Experimental

The experiment was conducted on the SSRF macromolecular crystallography beamline. The MarCCD was placed perpendicularly to the incident X-ray, with a surface area of 225 mm × 225 mm and pixel size of 73 μm × 73 μm. The X-ray was focused vertically and horizontally on the sample, in a high-flux and small spot, by a toroidal mirror. The diffraction spectra were collected by Debye-Scherrer method, and the  $1/\Delta 2\theta$  was determined by the  $p$ ,  $\alpha$ , and  $l$ . The slit to reduce scattering on the MarCCD was sized at 0.08 mm × 0.08 mm. The LaB<sub>6</sub> standard powder (NIST SRM 660a, 0.41569 nm) was stuck with deco glue to a Φ50 μm nylon loop, which did not affect the uniform distribution of diffraction pattern.

The wavelengths used in the experiments were 0.17433 (Fe), 0.16079 (Co), 0.13807 (Cu), 0.09795 (Se), and 0.06889 nm (Zr), and hundreds of saturation points were chosen as the exposure time. Fig.6 shows the diffraction patterns when the MarCCD is intersected by the Debye-Scherrer diffraction cone of the sample.

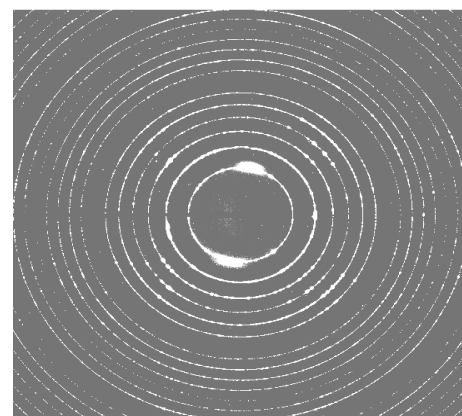


**Fig.6** Diffraction rings.

Diffraction patterns were obtained at absorption edges of Cu, Se and Zr in 7–18 keV, and diffraction patterns at the Zr absorption edge at different sample-to-MarCCD distances were collected to verify the energy calibration. Also, diffraction patterns at the Cu absorption edge were collected in exposure time of 5, 10, 15 and 20 s to check the exposure time effect on X-ray energy calibration. For the Zr K $\alpha$  X-ray (17.998 keV), the calibration error at the absorption edge was  $\pm 2$  eV at sample-to-MarCCD distances of 135–155 mm. This means that the calibration can be carried out quickly without adjusting the distance. In addition, the exposure time has no effect on the energy calibration: for the

calibrated energy Cu K $\alpha$  X-ray (8.980 keV) was 8.982–8.983 in calibration time of 5–20 s.

The EXAFS method was used to verify accuracy of the energy calibration. The calibration accuracy is  $\pm 1$  eV with 1 eV of step size of the monochromator. The larger flux of the odd number harmonics of the undulator, the sharper the peaks are, while the smaller flux of the even number harmonics of undulator, the gentler the peaks are. So the even harmonics were used to calibrate energy. With the 0.08 mm  $\times$  0.08 mm slit size of MarDTB for all the energy points, the calibration accuracy is within 3 eV in the whole range (Table 1). Note that the 1 and 2 means the first and second measurement.

**Table 1** Calibration at different energy points.

Actual energy / keV	7.112 (Fe)	7.709 (Co)	8.980 (Cu)	12.658 (Se)	17.998 (Zr)
Calibrated energy (1)	7.111	7.712	8.982	12.659	17.996
Calibrated energy (2)	7.112	7.712	8.983	12.661	18.000

#### 4 Conclusions

The X-ray beamlines of SSRF can be quickly calibrated *in-situ* without changing any beamline states, and this calibration method is suitable for other beamlines. The distance of the sample to MarCCD and the exposure time have little effect on the calibration accuracy. A more accurate calibration can be explored by multiple diffraction method.

#### References

- 1 Cross J O, Frenkel A I. Rev Sci Instrum, 1999, **70**: 38–40.
- 2 Acrivos J V, Hathaway K, Reynolds J, et al. Rev Sci Instrum, 1982, **53**: 575–581.
- 3 Arthur J. Rev Sci Instrum, 1989, **60**: 2062–2063.
- 4 Nicholas A, Rae, M, et al. Nucl Instrum Meth Phys Res, Sect. A, 2010, **619**:147–149.
- 5 Xu C L. Synchrotron Radiat Opt Eng 262–263.
- 6 Lu Q L, Min G H, Yu H S. Mater Rev, 2009, **19**: 5–7.
- 7 Norby P. J Appl Cryst, 1997, **30**: 21–30.
- 8 Appl J, Flemming R L. J Appl Cryst, 2005, **38**: 757–759.
- 9 Young R A, Wiles D B. J Appl Cryst, 1982, **15**: 430–438.